RERTR 2022 – 42ND INTERNATIONAL MEETING ON
REDUCED ENRICHMENT FOR RESEARCH AND TEST REACTORS

OCTOBER 3-5, 2022
VIENNA INTERNATIONAL CENTRE
VIENNA, AUSTRIA

NIST Neutron Source Preconceptual Design

Dağıstan Şahin, Osman Ş. Çelikten, Robert E. Williams, Jeremy C. Cook, Abdullah G. Weiss, Thomas H. Newton, David Diamond, Charles F. Majkrzak, Hubert E. King
NIST Center for Neutron Research
100 Bureau Drive, Gaithersburg, 20899, USA

Joy Shen, Anil Gurgen
Department of Mechanical Engineering
University of Maryland, College Park, MD 20742, USA

Eliezer Nahmani, Idan R. Baroukh
Nuclear Research Center Negev
P.O.B. 9001 84190, Beer-Sheva, ISRAEL

Lap-Yan Cheng
Nuclear Science & Technology Department
Brookhaven National Laboratory, P.O. Box 5000 Upton, NY 11973-5000, USA

This paper is dedicated to the memory of Robert E. Williams

ABSTRACT

The National Bureau of Standards Reactor (NBSR) at the NIST Center for Neutron Research (NCNR) provides a safe and reliable neutron source for the thousands of visiting U.S. and international researchers annually. A new state-of-the-art research reactor utilizing U-10Mo low-enriched uranium (LEU) monolithic fuel is being designed for the NCNR to replace the aging NBSR. The new reactor (NIST Neutron Source, or NNS) will be tailored primarily for neutron science involving thermal and cold neutron beams. This paper provides preconceptual design characteristics for the proposed NIST Neutron Source, highlights of reactor core neutronics and thermal-hydraulics analysis results, and a brief description of the user facilities, thermal neutron guides, cold neutron sources and cold neutron guide network. The initial results imply a total cold neutron current gain at the guide entrances ranging between a factor of 6.5 to 8.4, and at least a factor of two increase in the thermal neutron Maxwellian brightness with respect to the existing NBSR liquid hydrogen cold source.

1 Introduction

The NIST Center for Neutron Research (NCNR) houses the National Bureau of Standards Reactor (NBSR), which is one of the high performance research reactors in the U.S. and is the premier source of cold neutrons for thousands of visiting national and international researchers annually. The NBSR has a long history of successful operation since its startup in 1967 [1], and it is licensed to operate until 2029 at which point it will need to be relicensed. Currently, it is now one of only two major steady-state neutron scattering facilities in the U.S.

The NCNR has a long-standing reputation for scientific productivity, as measured by the abundance of scientific publications and number of research participants. The measurement facilities are perennially over-subscribed with a continually increasing demand from the scientific community. There are also increasing maintenance demands associated with the aging NBSR reactor systems and components. To address these issues in the longer term and to accommodate novel scientific instruments, a new state-of-the-art research facility is proposed for the NCNR. The new NIST Neutron Source, or NNS, will be tailored primarily for neutron science involving thermal and cold neutron beams. It will provide thermal neutron beams directly from the reactor core and cold neutron beams via cryogenically cooled moderator inserts (Cold Neutron Sources, or CNSs).

The proposed siting of the NNS adjacent to the NBSR would allow the latter to continue operation during the construction of the NNS and to share existing NCNR infrastructure and personnel resources. At initial startup (commissioning), the NNS would deliver equivalent measurement capabilities to the existing NBSR neutron source by operating minimum one cold source delivering cold neutrons to one of the guide halls. Once at full capacity, the facility would provide new measurement opportunities and should significantly alleviate the current over-subscription of scientific instruments by operation of both cold sources and guide halls.

With a primary focus on neutron beam experiments, an essential aspect of the proposed NNS user facility is the provision of cold and thermal neutron beams as well as several irradiation positions to meet the diverse needs of the neutron research community [2]. Cold neutrons have energies below about 5 meV [3], where the wave-particle duality of the neutron allows this range to be described by neutron wavelengths, λ, greater than about 0.4 nm. The challenge for neutron sources is to furnish collimated neutron beams of sufficient intensity to satisfy the demand for experimental throughput. The NNS intends to provide not only a replacement for an aging facility but aims to offer significantly increased scientific output through enhanced beam intensity and an expansion in the number of experimental stations available. This paper provides preconceptual design characteristics for the proposed NNS, highlights of the reactor core neutronics and thermal-hydraulics, and a brief description of the user facilities, thermal neutron guides, cold neutron sources and cold neutron guide network.

2 Design Description

The NNS reactor concept was influenced by several reactors designed for neutron science, particularly the Open Pool Australian Light Water (OPAL) reactor design, which were used extensively to ensure the use of realistic parameters for the preconceptual core and fuel assembly geometry [4]–[6]. The NNS is proposed to be an open-pool research reactor with a nominal power of 20 MW. It is composed of a light-water-cooled compact reactor core located inside a vertical channel (the "core chimney") that is surrounded by heavy-water in the reflector tank. These components/structures are located at the bottom of the reactor pool filled with demineralized light water.

The reflector tank encompasses the cold neutron sources and associated beam tubes as well as beam tubes for thermal neutron beams. The core is cooled by an upward flow of demineralized light water, which also acts as a neutron moderator. The core chimney channels the coolant to

outlet, where it is pumped away by the primary cooling system (PCS) for heat removal by the secondary cooling system. The PCS has four centrifugal pumps and four heat exchangers, each housed in separate rooms to lower common cause failures and allow maintenance, with only three units used for normal operation. The fourth pump and heat exchanger can either be in standby mode or under maintenance.

The general layout of the reactor including the PCS is shown in Figure 1. At the center of the figure (in yellow) is the reflector tank. The internals of the reflector tank, including the reactor core at the center, two cold neutron sources, and beam tubes are shown in Figure 2.

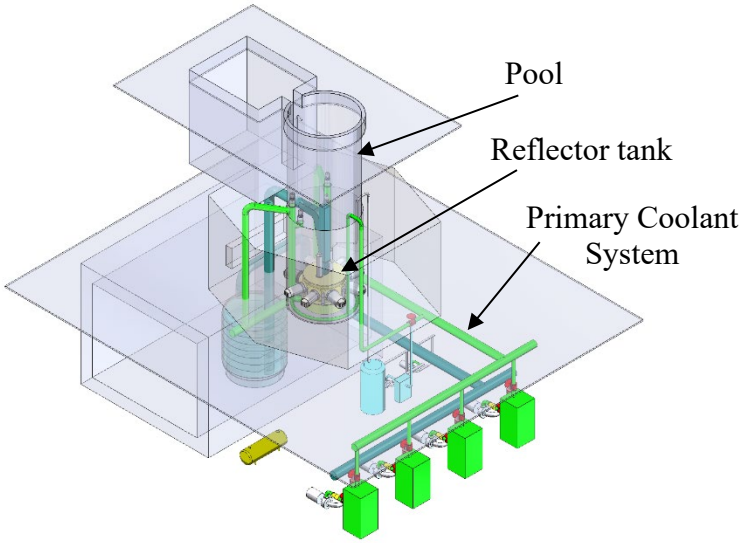

Figure 1: Reactor pool and primary coolant system

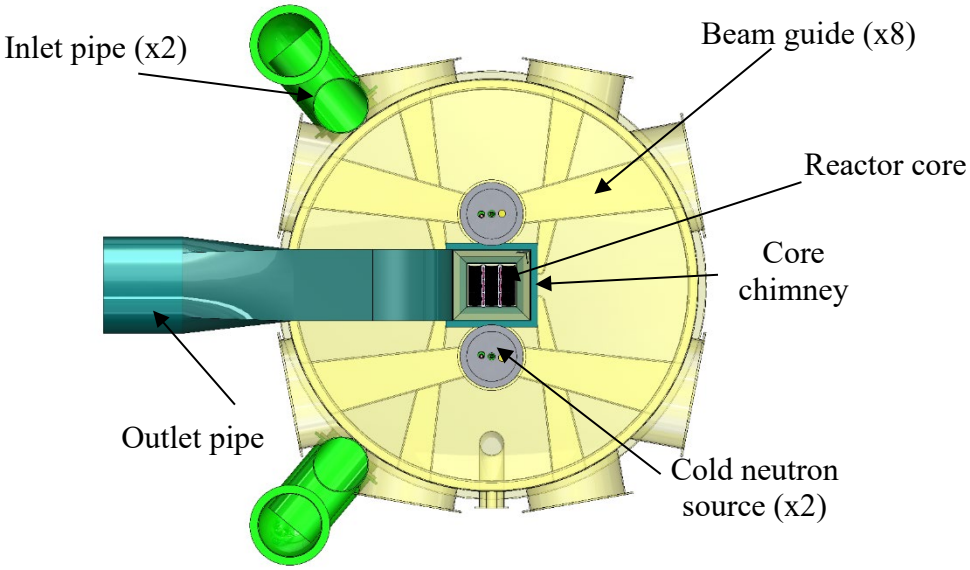

Figure 2: Reflector tank with core, cold sources, and beam tubes

3 Reactor Design and Neutronics

The NNS core consists of nine fuel assemblies (FAs) that are arranged in a 3x3 array, shown in Figure 3. There are six control blades placed in two guide boxes. The guide boxes divide the core into three rows; with 64 coolant channels at each row. Each fuel assembly, as seen in Figure 4, contains 21 urnium-10 wt.% molybdenum (U-10Mo) curved fuel plates (FPs) which are enriched to 19.75 wt.% U-235 with a ~8 μm thick zirconium foil interlayer to prevent chemical interactions

between the fuel and the Aluminum-6061 cladding [7], [8]. The two cold neutron sources are positioned on either side of the core per Figure 2. The core is designed to optimize the length of the fuel cycle and satisfy all thermal limits while maximizing peak thermal neutron flux in the reflector tank.

The two control blades adjacent to the central assembly are for control of reactivity during operation and the four other blades are shutdown or safety blades. The configuration shown in Figure 2 reflects the axial center of the core, whereas Figure 3 shows the core from a top view directly above the core. Figure 4 is a zoomed in view of a fuel assembly from above. Both control and safety blades are made of hafnium, which is selected for its increased longevity relative to cadmium blades currently used in the NBSR. To suppress the higher flux of the reactor at the initial stages of the fuel cycle, cadmium wires (0.5 mm diameter) are placed on each side of each fuel plate as a burnable poison. The cadmium wires slide into H_2O-filled T-shaped slots within the side plates of each assembly, where the water is used to provide some level of cooling for the cadmium wires.

In the neutronics model, using the MCNP code package [9], the fuel plates are assumed flat, fuel meat in each plate is discretized into axial and radial zones to account for spatial variations in the fuel composition and assist in equilibrium core computations. Axially, the fuel meat is discretized into 10 zones, where the top and bottom zones are 2-cm high, and the remainder are 8.25-cm high. Radially, the fuel is uniformly discretized into three zones each with a width of 2.167 cm. The thickness of the fuel plates is 0.25 mm.

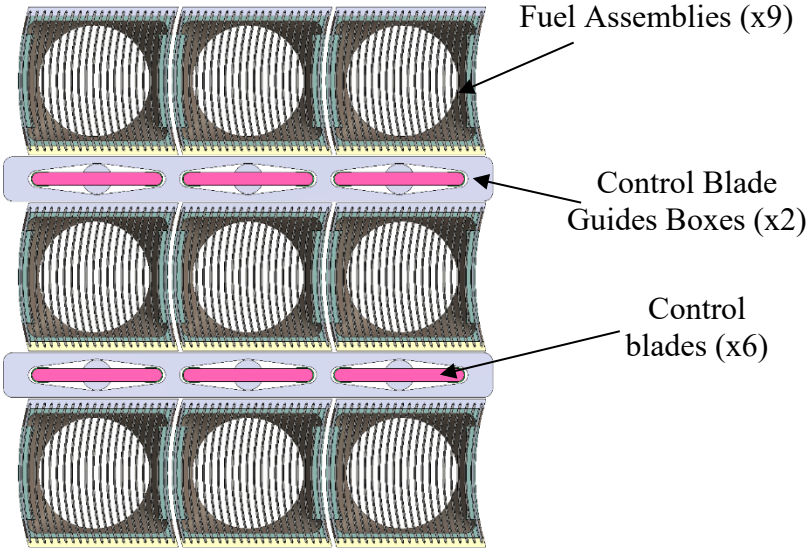

Figure 3: Pre-conceptual core design for the NNS

The NNS is designed to have a high leakage core, with multiple beam tube penetrations through the reflector and outer shielding. For neutron scattering experiments in particular, cold neutrons are useful, and they are obtained in the NNS using cryogenically cooled liquid deuterium-filled cold sources. Connected to the cold sources are cold neutron beam tubes made of zirconium alloy. Thermal neutron beam tubes, also made of zirconium, extend near the core and allow for out-of-core thermal neutron experiments. The presence of the cold neutron sources and beam tubes are important to understand the behavior of the core and is included in the MCNP models [10].

The power peaking factors at each fuel plate throughout the equilibrium core in the mid-plane are shown in Figure 5 at multiple cycle states, where the view and orientation of the core are consistent with Figure 3. The maximum generated power for each fuel assembly is calculated as 2.52 MW [10]. The highest power peaking occurs at the outer edges of the assemblies, which is a consistent finding throughout all cycle states. An assembly power of 2.37 MW and a 1.77 power peaking factor is obtained for the highest power plate during SU [10]. The outermost plates have more

power than the inner plates due to increased moderation (water) being present at the edges. This is consistent for all FAs in the core, but it is particularly prevalent in the FAs on the outer columns of the core (with respect to the views in Figure 3 and Figure 5).

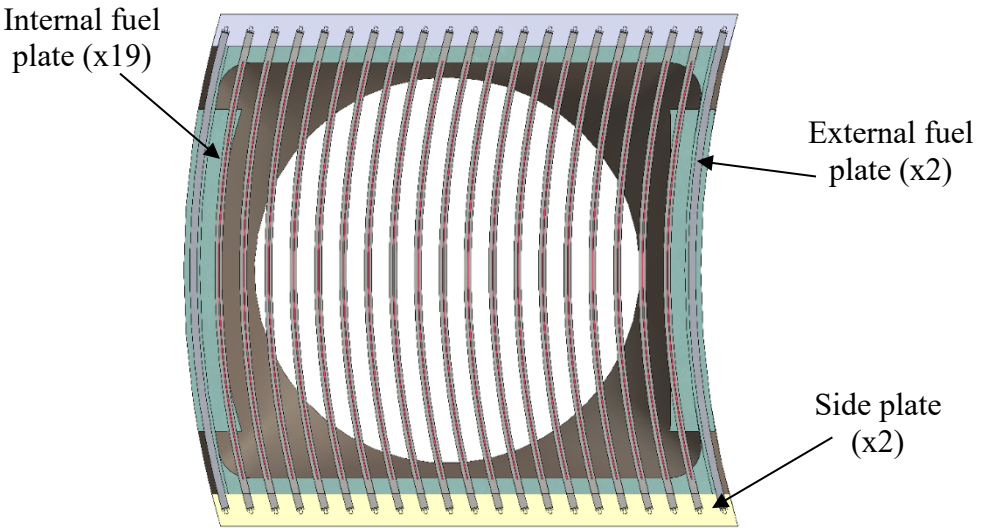

Figure 4: Single fuel assembly

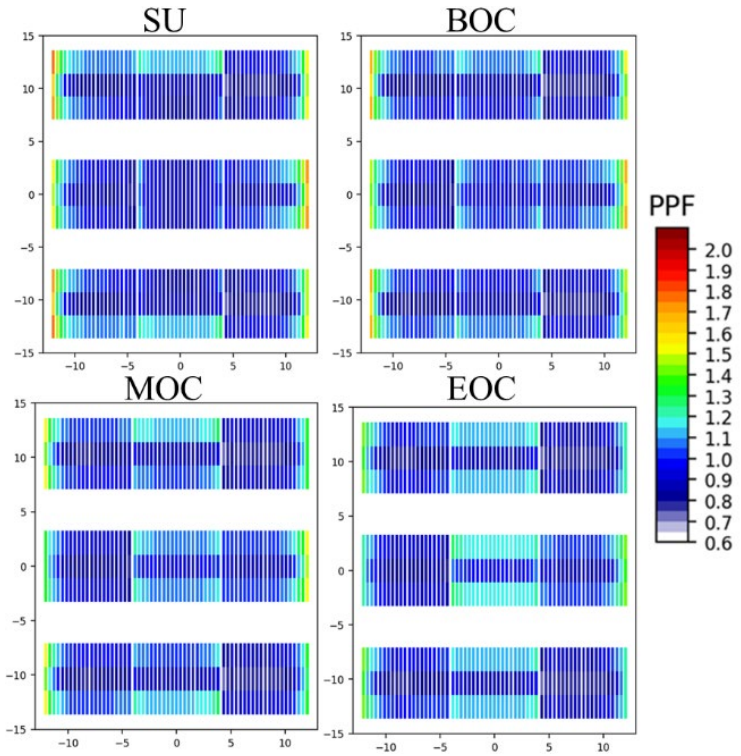

Figure 5: Spatial Distribution of the Power Peaking Factors at each Fuel Plate throughout the Core (SU=Start up, BOC=Beginning of Cycle, MOC=Middle of Cycle, EOC=End of Cycle)

Due to the implemented spatial power mesh discretization, the power and fission densities are calculated at 19,845 nodes throughout the equilibrium core. They are obtained at multiple equilibrium cycle states and for cycles transitioning to the equilibrium cycle spanning 40 days. These power and fission densities are illustrated in Figure 6 (a) for cycles 1-3 and Figure 6 (b) for

multiple cycle states. Note the presence of two additional cycle states in Figure 6 (b), such that the quarter 2 (Q2) and quarter 4 (Q4) states are used to cover the 2nd and 4th quarters of the 40-day cycle, respectively. Those two states are used as intermediate cycle states to eliminate most errors that arise from the constant location of control blades while moving from BOC to MOC or from MOC to EOC, respectively.

The lower fission densities in the 1st cycle are due to the freshly loaded cadmium absorber wires that effectively suppress the flux in early stages of operation. As the cadmium burnable poison is utilized, the maximum power density grows from around 16 kW/cm^3 in the 1st cycle to roughly 18 kW/cm^3. The maximum integral fission density similarly grows from around 1.5×10^{21} cm^{-3} in the 1st cycle to roughly 4.4×10^{21} cm^{-3} in the 3rd cycle [10].

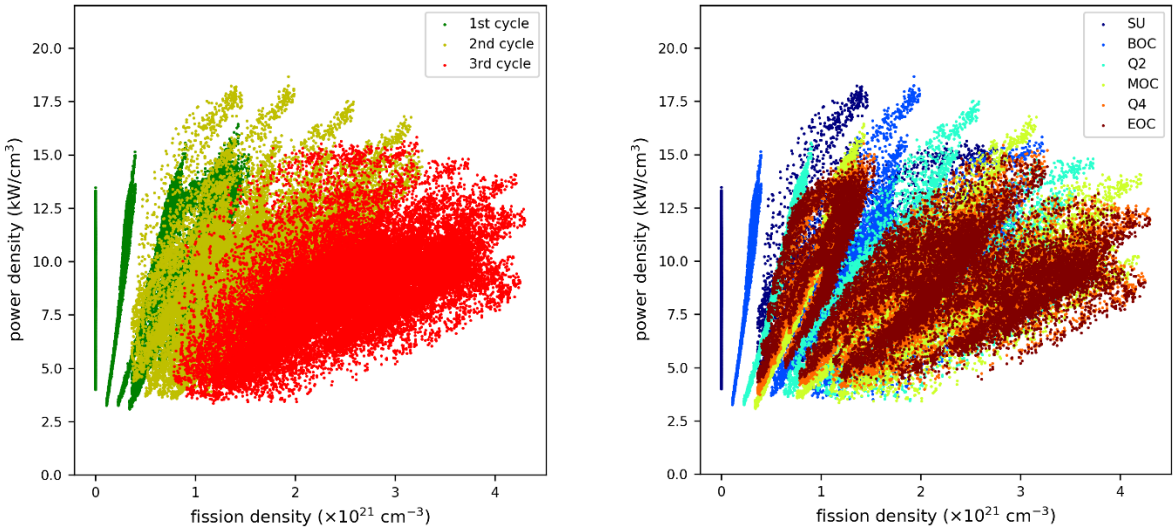

Figure 6: Distribution of the Correlation between Power and Fission Densities throughout the Core at (a) Multiple Cycles and (b) Multiple Cycle States

4 Core Thermal Hydraulics

The thermal-hydraulics model consists of a coupling between separate thermal and hydraulics models. The thermal model calculates the single-phase convective heat transfer between the fuel plates and the coolant, and it relies on pre-computed power distributions from the neutronics analysis. The model makes use of a one-dimensional energy balance formulae to calculate bulk coolant temperature and cladding wall temperature in each coolant channel, where the Petukhov and Kirillov correlation is used [11] to compute the heat transfer coefficient. The thermal model assumes symmetrical heat dissipation to the coolant channels and assumes a uniform power density within the fuel meat [12].

The hydraulics model calculates the flow distribution and pressure drop across the FAs by simulating parallel coolant channels that are connected to a shared inlet and shared outlet plenum, which means that the pressure drop across any given channel is the same. The diagram of all coolant channels in a single row with three FAs is given in Figure 7. It can be seen from the diagram that there are four different channel types in the hydraulics model, each denoted by a different color. Due to the curved nature of the fuel plates, the coolant channel between the chimney and the first FA is not equal to the one between the last FA and chimney. All the associated coolant channels are calculated considering the geometry specifications of the core.

The hydraulics model uses the pressure drop equation which is the integrated version of the one-dimensional momentum equation. For each coolant channel, the model computes the total

frictional pressure drop and local pressure drop at the entrance and exit of each channel as a function of the cell-average velocity and temperature. In order to calculate the friction factor, the Churchill correlation is used [13], [14].

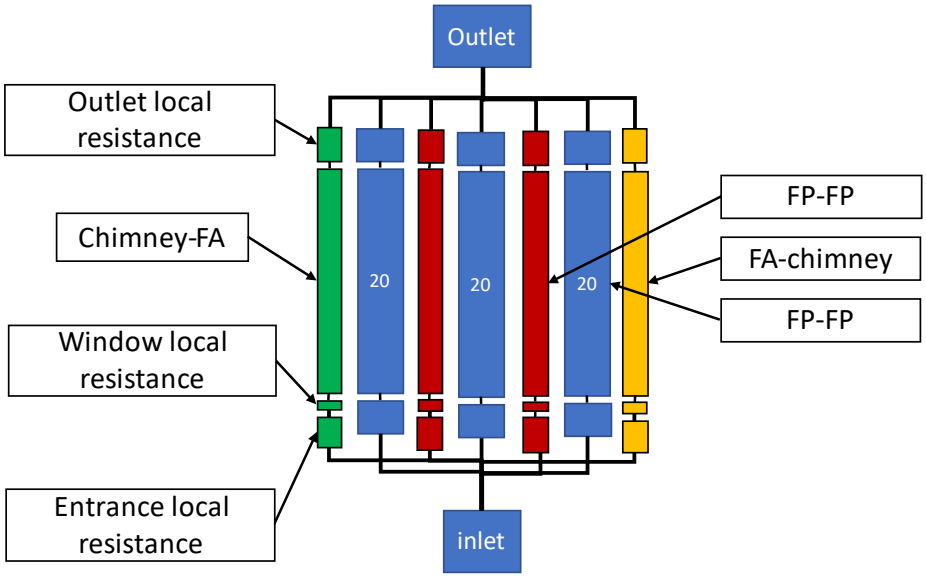

Figure 7: Diagram of Coolant Channels in FAs at a Single Row of the Core

Coupling the thermal and hydraulics models yields a consolidated model that solves for the reactor's thermal-hydraulics characteristics iteratively. In each iteration the thermal model calculates the bulk coolant temperature and cladding temperature for a given mass flow rate. Then the hydraulics model computes the pressure drop for the calculated temperatures and yields the mass flow rate distribution across all channels. The iterations are continued until the inlet and outlet mass flow rates converge to the pre-defined input value [12].
Cladding temperature distributions of selected fuel plates at startup (SU) are given in Figure 8 . The plot shows the axial cladding temperature distribution for the first (1), last (63), and some intermediate fuel plates (FP) in the bottom row (row C) including those at the interface of each FA. For SU, the highest cladding temperature is observed to be 361 K at the first FP of the bottom row. Other rows have very similar distributions across their FPs.

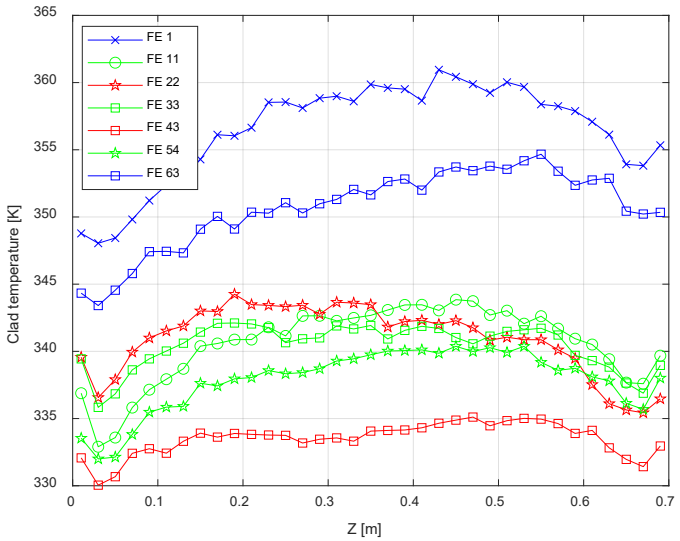

Figure 8: Axial Temperature Distributions of Cladding Walls of Different FPs in a Row at SU

The thermal limits for different core states are given in Table 1, where the critical heat flux needed to compute the minimum critical heat flux ratio (mCHFR) is obtained using the Sudo-Kaminaga correlation [15]. The onset of flow instability ratio (OFIR) is computed using the Saha-Zuber correlation [16]. Across all core states, the core maintains a relatively stable mCHFR and OFIR, which increases as the core proceeds through its cycle. The mCHFR is always greater than 2, which agrees with the general acceptance provided by the U.S. Nuclear Regulatory Commission in NUREG 1537 [17].

Table 1: Thermal Limits at Different Core States

Core State	mCHFR	OFIR
SU	2.22	12.9
BOC	2.18	13.6
MOC	2.42	15.2
EOC	2.61	15.1

5 Neutron Guides, Instrumentation and Facilities

The NNS reactor core and CNS design prioritizes a significant increase in the useable cold neutron beam intensity relative to the NBSR. All neutron guides shown are technically feasible and to scale. Each has a high simulated cold neutron transmission using currently available supermirror coatings combined with a low fast-neutron and gamma-ray transmission (due to the guide curvature). Definitions of the instruments are summarized in Table 2. Further details are given in Ref. [2]. Additional end-guide positions can be created with benders on guides whose end-position instruments do not require the full beam height (e.g., SANS instruments). Monochromatic beam positions may be created on the sides of the longer guides and on outer guides where the full beam area can be used in most cases with little perturbation to downstream instruments.

Table 2: Proposed Cold Neutron Instruments for the Guide Halls

Instrument Type	Total Number	End Position
Small-Angle Neutron Scattering (SANS)	2-3	YES
Reflectometer (CANDOR type)	2	YES
Cold Neutron Imaging (CNI)	2	YES
Cold 3-Axis (CN3X)	2	YES
Backscattering (BS)	2	YES/NO?
Neutron Spin-Echo (NSE) (Mezei-type)	1	YES
Neutron Spin-Echo (NSE) (WASP type)	1	YES
High current physics experimental position (Physics)	1	YES
Prompt Gamma Activation Analysis (PGAA)	1	YES
Neutron Depth Profiling (NDP)	1	YES
Materials Diffractometer ($\lambda > 0.3$ nm)?	1?	YES
Interferometer	1?	NO
Monochromatic Physical Measurements Laboratory (PML) positions	2-3?	NO
Miscellaneous monochromatic/ test positions	2-3?	NO
Very Small-Angle Neutron Scattering (vSANS)	1	YES
TOTAL	22-25	16-18

Instruments being considered for use on the thermal beams, along with their abbreviations, are listed in Table 3. Thermal beam instruments are considered as one of each where the number of instruments could be adjusted based on scientific need. Accommodating a possible suite of nine thermal beam instruments at the NNS will likely require several instruments being located further from the core on neutron guides. These may be straight or curved multichannel “bender” devices.

As for the cold neutron instruments, the thermal neutron instrument suite will be finalized in collaboration with the user community.
The NNS will produce a significant gain in thermal neutron flux by having a compact core design. The NBSR, which by contrast has a larger cross-sectional area, has a peak unperturbed thermal neutron flux in the reflector of about 2×10^{14} $cm^{-2}s^{-1}$ at a 20 MW power level. The NNS core will produce a minimum peak unperturbed thermal neutron flux in the reflector of about 5×10^{14} $cm^{-2}s^{-1}$ at 20 MW [10].

Table 3: Instruments being considered for the NNS Thermal Beams

Instrument Type	**Abbreviation**
Prompt Gamma Neutron Activation Analysis	PGNAA
Neutron Microscope	Imaging
High-Resolution powder diffractometer	D
Triple Axis Spectrometer	3X
Ultra-Small Angle Neutron Scattering	USANS
High Throughput Fast Powder Diffractometer	D
White Beam Engineering Diffractometer (with CANDOR-type detector)	ENG
High Current Physics Experimental Position	PHYS

6 Discussion and Future Work

The preconceptual design characteristics for the proposed NNS, highlights of the reactor core neutronics, thermal-hydraulics analysis results showing the feasibility and safety of the compact design are provided in this paper. Based on neutronic analysis, power peaking factors, integral fission densities and core cycle length were found to be acceptable. Furthermore, based on thermal hydraulic calculations, the mCHFR is found to be always greater than 2 at any core state. Future work includes neutronic, thermal hydraulic, structural, and material analysis, along with optimization studies to improve the core design. Additionally, other fuel options, such as uranium silicide, are to be evaluated for performance and safety evaluations.
By having two major CNSs the NNS increases cold neutron guide access with a broad suite of cold neutron instruments and an increased number of cold-neutron end-stations. Extensive simulations have been performed [2], [18] which compare the NBSR existing Unit 2 liquid hydrogen (LH_2) CNS with the NNS dual LD_2 CNSs. The initial results imply a total cold neutron ($\lambda > 0.4$ nm) current gain at the guide entrances ranging between 6.5 and 8.4, depending on the choice of guide entrance cross-section [18]. There are indications that these gain factors could increase with further optimization of the CNS dimensions. The cold neutron gain at the instruments may be further enhanced over that available at the guide entrances by designing the intervening neutron optics for improved transmission within the specific beam area, beam divergence, and bandwidth used by the instruments. Moreover, it is planned that the design of each individual instrument be optimized for performance, employing as many advanced concepts and state-of-the-art neutron optical components as possible. Such improvements, along with the high brightness of dual CNSs creates a potential for a significant boost in the cold neutron experimental output over what is currently possible at the NCNR.

7 Disclaimer

Certain commercial equipment, instruments, or materials are identified in this study in order to specify the experimental procedure adequately. Such identification is not intended to imply recommendation or endorsement by the National Institute of Standards and Technology, nor is it intended to imply that the materials or equipment identified are necessarily the best available for the purpose.

8 References

[1] J. J. Rush and R. L. Capelleti, *The NIST Center for Neutron Research: Over 40 Years Serving NIST/NBS and the Nation*. National Institute for Standards and Technology, 2011.

[2] J. C. Cook *et al.*, "Proposed NIST Neutron Source User Facility," *ANS Winter Meet. 2022 Ariz. USA*, vol. In Press.

[3] F. J. Webb, "Cold neutron sources," *J. Nucl. Energy Parts AB React. Sci. Technol.*, vol. 17, no. 4, pp. 187–215, Jul. 1963, doi: 10.1016/0368-3230(63)90021-1.

[4] G. Braoudakis, "OPAL nuclear reactor: Reactor specification," vol. 46, no. 20, Feb. 2015, Accessed: Jun. 09, 2021. [Online]. Available: http://inis.iaea.org/Search/search.aspx?orig_q=RN:46046717

[5] S. J. Kennedy, "Construction of the neutron beam facility at Australia's OPAL research reactor," *Phys. B Condens. Matter*, vol. 385–386, pp. 949–954, Nov. 2006, doi: 10.1016/j.physb.2006.05.280.

[6] S.-J. Kim, "The OPAL (open pool Australian light-water) reactor in Australia," *Nucl. Eng. Technol.*, vol. 38, no. 9, pp. 443–448, 2006.

[7] A. B. Robinson, G. S. Chang, J. Keiser, D. M. Wachs, and D. L. Porter, "Irradiation Performance of U-Mo Alloy Based 'Monolithic' Plate-Type Fuel – Design Selection," Idaho National Lab. (INL), Idaho Falls, ID (United States), INL/EXT-09-16807, Aug. 2009. doi: 10.2172/968567.

[8] D. J. Turkoglu, Z. Wu, R. E. Williams, and T. H. Newton, "Comparison of Neutronics Performance Characteristics of the Proposed NIST Reactor with different LEU Fuels," presented at the PHYSOR 2018: Reactor Physics Paving the Way Towards more Efficient Systems, Cancun, 2018.

[9] C. J. Werner *et al.*, "MCNP Users' Manual Code Version 6.2," Los Alamos National Laboratory, LA-UR-17-29981, Sep. 2017. Accessed: Jul. 07, 2021. [Online]. Available: https://mcnp.lanl.gov/pdf_files/la-ur-17-29981.pdf

[10] O. S. Celikten, D. Sahin, and A. G. Weiss, "Highlights of Neutronics Analyses for the Pre-conceptual NIST Neutron Source Design," *ANS Winter Meet. 2022 Ariz. USA*, vol. In Press.

[11] B. S. Petukhov and V. V. Kirillov, "On the Question of Heat Transfer to a Turbulent Flow of Fluids in Pipes," *Tepl. Therm. Eng.*, vol. 4, pp. 63–68, 1958.

[12] I. R. Baroukh, A. Gurgen, J. S. Shen, and A. G. Weiss, "A Preliminary Thermal-hydraulics Analysis for the NIST Neutron Source," *ANS Winter Meet. 2022 Ariz. USA*, vol. In Press.

[13] F. White, *Fluid Mechanics*, 7th Ed. McGraw-Hill Series in Mechanical Engineering, 2009.

[14] S. W. CHURCHILL, "Friction-factor equation spans all fluid-flow regimes," *Chem. Eng.*, vol. 84, no. 24, pp. 91–92, 1977.

[15] M. Kaminaga, K. Yamamoto, and Y. Sudo, "Improvement of Critical Heat Flux Correlation for Research Reactors using Plate-Type Fuel," *J. Nucl. Sci. Technol.*, vol. 35, no. 12, pp. 943–951, 1998, doi: 10.1080/18811248.1998.9733966.

[16] P. Saha and N. Zuber, "Point of Net Vapor Generation and Vapor Void Fraction in Subcooled Boiling," in *Proceeding of International Heat Transfer Conference 5*, Tokyo, Japan, 1974, pp. 175–179. doi: 10.1615/IHTC5.430.

[17] Nuclear Regulatory Commission, Washington, DC (United States). Office of Nuclear Reactor Regulation, "Guidelines for preparing and reviewing applications for the licensing of non-power reactors: Standard review plan and acceptance criteria.," NUREG-1537 Pt.2, 211545, Feb. 1996. doi: 10.2172/211545.

[18] J. C. Cook *et al.*, "Neutron Delivery Systems Design of the Proposed NIST Neutron Source," *ANS Winter Meet. 2022 Ariz. USA*, vol. In Press.

.